

**FINAL REPORT**

**TESTING OF SELECTED METALLIC REINFORCING BARS FOR EXTENDING  
THE SERVICE LIFE OF FUTURE CONCRETE BRIDGES:  
TESTING IN OUTDOOR CONCRETE BLOCKS**

**Gerardo G. Clemeña, Ph.D.**  
**Research Scientist**  
**Virginia Transportation Research Council**

**Y. Paul Virmani, Ph.D.**  
**Program Manager**  
**Office of Infrastructure Research and Development**  
**Turner-Fairbank Highway Research Center**  
**Federal Highway Administration**

Virginia Transportation Research Council  
(A Cooperative Organization Sponsored Jointly by the  
Virginia Department of Transportation and  
The University of Virginia)

In Cooperation with the U.S. Department of Transportation  
Federal Highway Administration

Charlottesville, Virginia

December 2002  
VTRC 03-R6

## **DISCLAIMER**

The contents of this report reflect the views of the authors, who are responsible for the facts and the accuracy of the data presented herein. The contents do not necessarily reflect the official views or policies of the Virginia Department of Transportation, the Commonwealth Transportation Board, or the Federal Highway Administration. This report does not constitute a standard, specification, or regulation.

Copyright 2002 by the Commonwealth of Virginia.

## ABSTRACT

To meet the challenge of a design life of 100 years for major concrete bridges, economical and corrosion-resistant reinforcing bars will be needed. The preliminary results for stainless steel-clad bars in a recent investigation funded by the Federal Highway Administration suggested that stainless steel-clad bars could qualify.

To verify these results, this investigation compared the behavior of clad bars, three solid stainless steel (316LN, 304, and 2205) bars, and the traditional carbon steel bars in test concrete blocks exposed to weekly cycles of ponding with a saturated salt solution and drying. Regular measurements of electrochemical parameters such as macrocell current, corrosion rate, and open-circuit potential throughout the first 700 days of exposure indicated that the clad bars and the three solid stainless steel bars have virtually the same excellent resistance to corrosion. Whereas the carbon steel bars started to corrode after only 90 days of exposure, the other bars did not evidence any discernible corrosion activity, even after 700 days. A comparison of the estimated chloride concentrations at 90 and 700 days indicated that the clad bars and the stainless steel bars could tolerate at least 15 times more corrosive chloride ions than could the carbon steel bars.

## **FINAL REPORT**

### **TESTING OF SELECTED METALLIC REINFORCING BARS FOR EXTENDING THE SERVICE LIFE OF FUTURE CONCRETE BRIDGES: TESTING IN OUTDOOR CONCRETE BLOCKS**

**Gerardo G. Clemeña, Ph.D.**  
**Research Scientist**  
**Virginia Transportation Research Council**

**Y. Paul Virmani, Ph.D.**  
**Program Manager**  
**Office of Infrastructure Research and Development**  
**Turner-Fairbank Highway Research Center**  
**Federal Highway Administration**

## **INTRODUCTION**

The life of any concrete bridge exposed to the chloride ions present in deicing salt or seawater can be significantly limited by concrete deterioration caused by corrosion of the carbon steel reinforcement. The combined use of concrete with a low water-to-cement ratio, thicker concrete cover, and epoxy-coated bars by many transportation agencies since the early 1980s has, in general, been successful in delaying the onset of rebar corrosion in many states such that many of these bridges will likely reach or even exceed their 50-year design life. Now, with highway construction costs rising higher every year, by 12 percent annually since 1987, transportation agencies must do everything possible to ensure that future highways and bridges will last even longer. To their credit, these agencies have set goals of at least 75 years for minor bridges and at least 100 years for major bridges. Achieving these goals will require either major improvements to the current coated bars or the development of a new bar, one that is not only intrinsically more corrosion resistant but also reasonably affordable.

Aimed at finding such a bar, the Federal Highway Administration (FHWA) recently sponsored an investigation in which many types of experimental bars were subjected to cycles of immersion in salt solutions of various concentrations and drying.<sup>1</sup> In this study, bars made of stainless steels (304, 316, and nitronic 33), which are well known for their good corrosion resistance in many other applications, were associated with corrosion rates 100 to 750 times less than those of carbon steel bars. An independent evaluation of bars made of stainless steel 304 and 316 found that the chloride corrosion thresholds of these materials were at least 12 times higher than that of carbon steel bars.<sup>2</sup> These encouraging results indicated that stainless steel bars would be able to withstand attack by high concentrations of chloride and, therefore, allow bridges built with them to last considerably longer than even those built with epoxy-coated carbon steel bars. However, the average cost of stainless steel bars is prohibitively high: approximately 5 times that of epoxy-coated carbon steel bars (excluding installation cost).

The FHWA-funded study also examined a carbon steel bar clad with stainless steel, albeit on a preliminary basis because of the lack of test samples of sufficient quantity at that time, and found that the bar can have the same corrosion resistance as the solid stainless steel bars investigated.<sup>1</sup> Since this bar can be produced and sold at a significantly lower cost than any of the solid stainless steel bars, at less than a half, the bar appeared to be promising in the quest to achieve the new design-life goals. The potential of a huge market prompted a company in the United Kingdom to venture into the manufacture of clad bars, using its patented processes. Following this lead, a U.S. manufacturer of steel bars set up a new plant to produce clad bars in the late autumn of 2002 using a unique cladding process. These commercial developments are expected to lead to price competition, or at least stability, which would benefit highway agencies.

## **PURPOSE AND SCOPE**

The prospect of significantly extending the service life of future concrete bridges and thereby realizing tremendous savings in the future for many transportation agencies led to this investigation to verify the good corrosion resistance of clad bars. The corrosion resistance of clad bars was compared with that of conventional carbon steel bars and three solid stainless steel bars in test concrete blocks subjected to accelerated salt exposure.

Since there was a likelihood that this approach to testing the bars might not yield discernible results within the scheduled 2-year time frame of this study, comparative tests of some of these materials were also conducted in simulated concrete pore solutions of different pH and salt concentrations. Although testing in such solutions could not perfectly simulate the bar-to-concrete interface conditions to which reinforcing bars are subjected in concrete, the approach provided a quick and relative sensitive way to compare these materials. The results obtained from the solution testing of the different materials are presented elsewhere.<sup>3</sup> This report presents the results obtained from the comparative testing conducted in concrete.

## **METHODOLOGY**

### **Reinforcing Bars Tested**

In addition to a stainless steel-clad carbon steel bar (Figure 1), bars made of the following materials were tested: (1) the widely used carbon steel (ASTM A 615M), (2) a solid AISI 316LN stainless steel, (3) a solid AISI 304 stainless steel, and (4) a duplex 2205 stainless steel. Both straight and U-bent bars of each material were used in the investigation. The clad bars from the United Kingdom had a nominal diameter of 19 mm, and the other bars had a nominal diameter of 16 mm. The average thickness of the stainless steel cladding on the clad bars was 1.08 mm, with a standard deviation of 0.23 mm. The minimum and maximum thickness was 0.44 mm and 1.43 mm, respectively. To assess the possible effects of damage in the stainless steel cladding on the carbon steel core, two holes 3 mm wide were drilled through the cladding in each of several randomly selected clad bars to expose the carbon steel core before

it was embedded in concrete. With this exception, the bars were tested in the same condition in which they were received.



**Figure 1. Stainless Steel–Clad Bars Obtained From Stelax UK Limited, West Glamorgan, U.K.**

### Test Concrete Blocks and Their Accelerated Exposure to Salt

The bars were embedded in concrete blocks (Figures 2 and 3) in various combinations to form the test matrix provided in Table 1. In some subsets of blocks, only the stainless steel bars or the clad bar was used in the top of the blocks and the carbon steel bars were used in the bottom. This was to reflect the situation in which a bridge deck owner decides to use such a

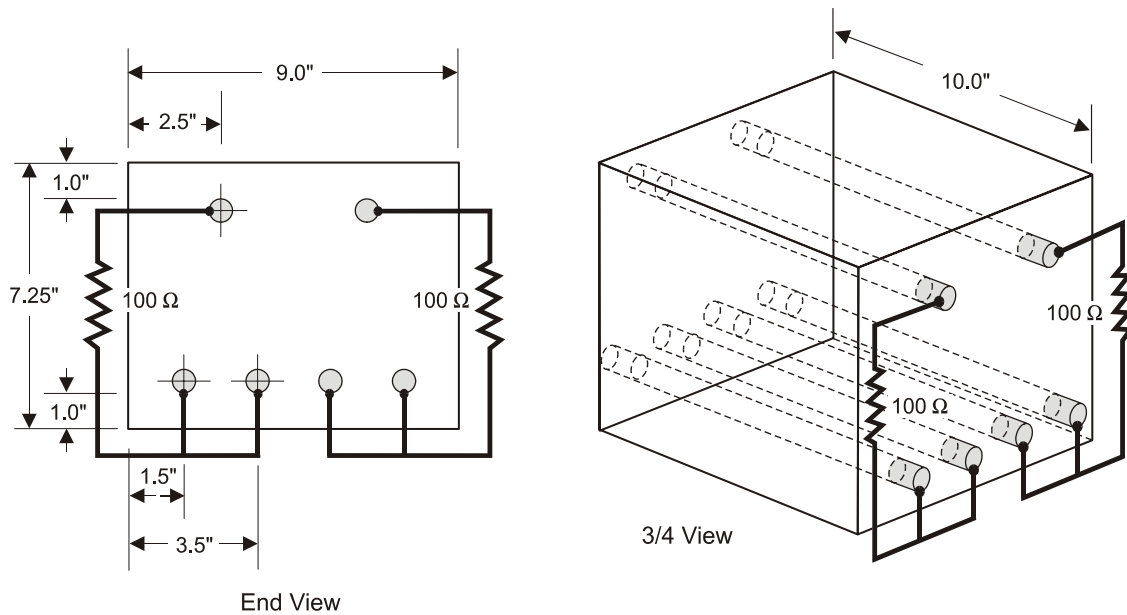


**Figure 2. Test Concrete Blocks With Straight Bars in Top Portion (1.0 in = 25.4 mm).**

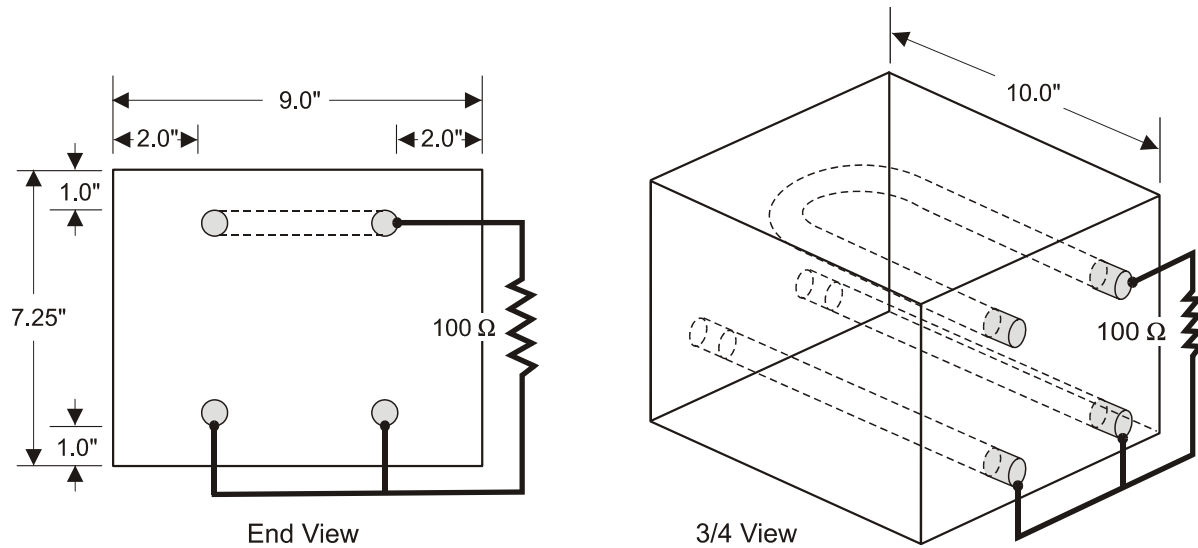


Figure 3. Test Concrete Blocks with U-bent Bars in Top Portion (1.0 in = 25.4 mm).

Table 1. Test Matrix

Bar	Bar Combination		No. of Blocks	Block Designation
	Top Mat	Bottom Mat		
Carbon Steel	Carbon Steel–Straight	Carbon Steel–Straight	4	CS/CS
	Carbon Steel–Bent	Carbon Steel–Straight	8	CS (bent)/CS
316LN	316LN–Straight	316LN–Straight	4	316LN /316LN
	316LN–Straight	Carbon Steel–Straight	4	316LN/CS
	316LN–Bent	Carbon Steel–Straight	8	316LN (bent)/CS
304	304–Straight	304–Straight	4	304/304
	304–Straight	Carbon Steel–Straight	4	304/CS
	304–Bent	Carbon Steel–Straight	8	304 (bent )/CS
2205 Duplex	2205 Duplex–Straight	2205 Duplex–Straight	4	2205/2205
	2205 Duplex–Straight	Carbon Steel–Straight	4	2205/CS
	2205 Duplex–Bent	Carbon Steel–Straight	8	2205 (bent)/CS
Clad Bar	Clad Bar–Straight	Clad Bar–Straight	4	CB/CB
	Clad Bar–Straight (w/holes)	Clad Bar–Straight	4	CB (w/holes)/CB
	Clad Bar–Straight	Carbon Steel–Straight	4	CB/CS
	Clad Bar–Bent	Carbon Steel–Straight	8	CB (bent)/CS

CS = carbon steel bars; CB = clad bars.

combination of bars (i.e., a more expensive but more corrosion-resistant bar in the top mat and a cheaper but less corrosion-resistant bar in the bottom mat) to reduce cost. A few days after the concrete blocks were fabricated using the concrete mixture described in Table 2, a wooden dam was built on the top surface of each block. Then, the blocks were allowed to cure outdoors for approximately 30 days before their sides were coated with epoxy. Immediately after, the blocks were subjected to weekly cycles of ponding for 3 days with a saturated solution of NaCl followed by drying for 4 days.

**Table 2. Concrete Mixture Used for Test Blocks**

Parameter	Value
Water-to-cement ratio (w/c)	0.50
Type II cement (kg/m <sup>3</sup> )	390
Stone (kg/m <sup>3</sup> )	1059
Sand (kg/m <sup>3</sup> )	828

### Measurements Made on Test Concrete Blocks

Measurement of the macrocell current that might be flowing between the top and bottom bars in each block was started at almost the same time as the ponding and continued almost weekly throughout the study. The macrocell current was determined by measuring the voltage drop across a 100-ohm resistor connected between each top bar and its two corresponding bottom bars using a high-impedance multimeter with the negative terminal connected to the bottom bars. In this manner, a negative voltage drop corresponds to a positive macrocell (galvanic) current, i.e., the top bars are anodic in comparison to the bottom bars. Since the diameters of all types of bars were not the same, each measured macrocell current was normalized by dividing it by the estimated surface area of the corresponding top reinforcing bar inside a concrete block. No assumption was made that any corrosion activity that might be occurring on a bar was uniformly distributed across its entire embedded surface. The estimated error of measurements for the macrocell current was  $\pm 0.10 \mu\text{A}$ , or in terms of normalized macrocell currents was  $\pm 0.0008 \mu\text{A}/\text{cm}^2$ . Finally, the normalized macrocell currents for all concrete blocks in each subset were averaged to yield the subset's mean macrocell current.

Measurements of the polarization resistance and open-circuit potential of each of the top bars in each concrete block were also conducted using a Cortest Instrument PR Monitor that used a guard ring to better define the bar area being polarized during a test. During each measurement, the guard-ring probe assembly was placed directly over the piece of top bar being measured and at the center of the bar (along its length). If the top bar was a U-bent bar, the probe assembly was placed directly over the entire bent section of the bar. A Cu/CuSO<sub>4</sub> electrode (CSE) was used as the reference electrode. From the measured polarization resistance ( $R_p$ ), the corrosion rate ( $I_{corr}$ ) of a piece of top bar was calculated using the Stern-Geary equation:

$$I_{corr} = \frac{\beta_a \beta_c}{2.3(\beta_a + \beta_c)} \frac{1}{A} \frac{dI}{dE} = \frac{\beta_a \beta_c}{2.3(\beta_a + \beta_c)} \frac{1}{AR_p} \quad (1)$$

where  $\beta_a$  and  $\beta_c$  are the anodic and the cathodic Tafel coefficient, respectively;  $A$  is the surface area of a bar being polarized; and  $dI/dE$  is the slope at the corrosion potential of an  $E$ -vs- $I$  curve. The surface area is that of the section of a top straight or U-bent bar directly underneath the guard-ring probe assembly. Similarly, the corrosion rates of all individual top bars in the same group of material or test concrete blocks were then averaged.

The concentrations of the chloride ions in 10 randomly selected concrete blocks (2 from each of the five groups of blocks) were determined at three times (168, 299, and 453 days) after the initiation of the salt exposure regime. At each sampling time, pulverized concrete samples were extracted from each block at three depths. The samples were then analyzed for their (total) chloride contents in accordance with the standard procedures described in AASHTO T-260.

## RESULTS AND DISCUSSION

### Macrocell Currents

Corrosion of reinforcing steel bars in concrete is basically galvanic in nature. It is caused by the presence of electrochemical cells on the surface of the steel bars, each of which consists of an anodic and a cathodic area. The cells are referred to as microcells when the anodic and cathodic areas are uniformly distributed across a section of a bar. If instead the anodic and cathodic areas are remote from each other and exist on a single piece of bar or adjacent bars that are in electrical contact, such as bars in the same mat or in a bridge deck in two different mats, the cells are referred to as macrocells. Both types of corrosion cells are created by the existence of differences in the condition in the concrete (such as chloride ion, oxygen, and moisture contents; pH; and contact between the steel surface and the concrete), which are consequences of the heterogeneous nature of concrete, and differences in the surface condition of the metallic bars.

It has been suspected that in concrete bridge decks, where there are typically two mats of reinforcing bars (one at a deeper level than the other) and the ingress of the deicing salts is typically from the top surface of the deck so that the top mat of reinforcing bars is normally exposed to more chloride ions, macrocells are the major driving force of corrosion. This leads to the all-too-familiar corrosion of the top reinforcing bars and the resulting delamination of the surrounding concrete in concrete bridge decks. The design of the test concrete blocks and the manner in which they were exposed to salt were intended to simulate this type of situation in this type of concrete structure.

Figure 4 shows the mean macrocell currents of the two subsets of concrete blocks that were reinforced with carbon steel bars at the top and bottom portions, i.e., CS/CS and CS (bent)/CS, while these blocks were being subjected to weekly cycles of ponding and drying. For the CS/CS blocks, even from the very beginning of the salt-exposure regime, there was already a discernible macrocell current, which is an indication of corrosion activity. The direction of the current indicated that the top carbon steel bars were anodic to the bottom bars. The current was as much as  $0.182 \mu\text{A}/\text{cm}^2$  at day 26, followed by a brief decline through day 95. Then, after a plateau between days 95 and 120, the macrocell current began to rise steadily (with the exception of fluctuations caused by changing outdoor conditions). For the first 700 days, the average macrocell current for the entire set of concrete blocks reinforced with straight carbon steel bars at the top was  $0.414 \mu\text{A}/\text{cm}^2$  (Table 3).

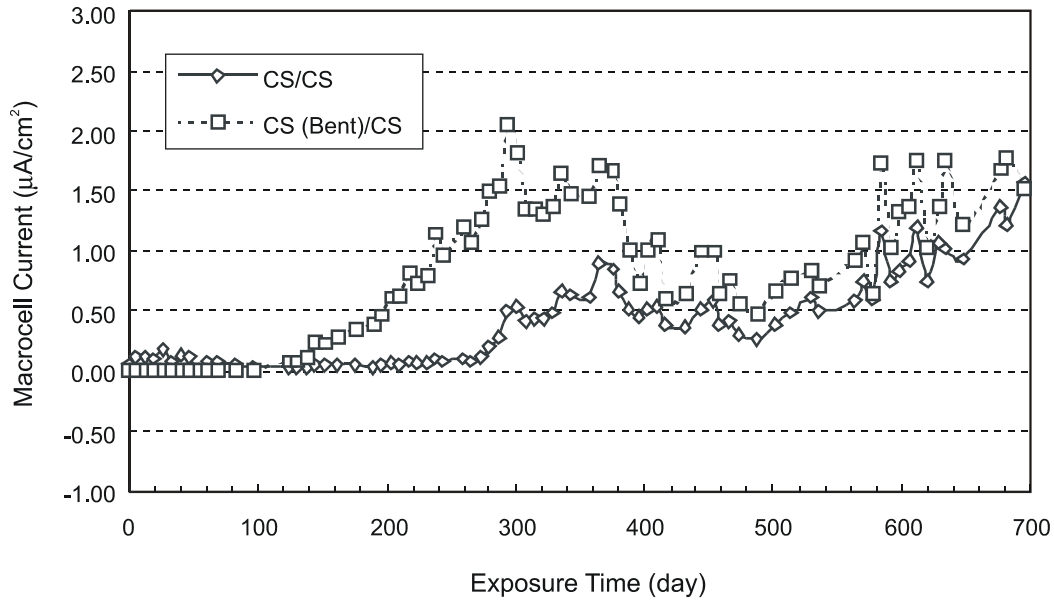


**Figure 4. Macrocell Currents of Test Concrete Blocks With Either Straight or Bent Carbon Steel Bars in Top.** The macrocell currents were normalized to the surface area of the top bars in the concrete blocks.

**Table 3. Macrocell Currents Densities for Various Groups of Test Concrete Blocks**

Test Blocks	Mean Macrocell Current ( $\mu\text{A}/\text{cm}^2$ ) <sup>a</sup>
CS/CS	0.414 ± 0.0008
CS (bent)/CS	0.857
316LN/316LN	0.0000
316LN/CS	-0.0038
316L (bent)/CS	-0.0031
304/304	-0.0002
304/CS	-0.0026
304 (bent)/CS	-0.0004
2205/2205	0.0004
2205/CS	-0.0286
2205 (bent)/CS	-0.0058
CB/CB	0.0000
CB (w/holes)/CB	-0.0001
CB/CS	-0.0077
CB (bent)/CS	-0.0109

CS = carbon steel bars; CB = clad bars.

<sup>a</sup>The sign indicates the direction of current flow between the top and bottom mats.

Interestingly, the mean macrocell current of the CS (bent)/CS blocks, i.e., with bent carbon steel bars in the top portion, was practically indiscernible throughout the first 90 days of exposure (almost 13 exposure cycles), indicating that the top bars were initially passive. Then, the bars began to corrode, as indicated by the rapid rise in the macrocell current, at a rate that exceeded that of the blocks with the straight carbon steel bars and eventually reached a rate several times higher. The cause for this large difference in magnitudes of the macrocell currents

is uncertain; it might be attributable to an unknown difference in the surface conditions of the two groups of bars (of the same material), which perhaps resulted from bending. Noteworthy is that after approximately 400 days, the magnitude of the macrocell currents of the blocks with straight carbon steel bars had almost reached that of those with bent carbon steel bars (Figure 4).

The fluctuations in the macrocell currents for these two sets of blocks generally reflected changes in the outdoor exposure conditions (temperature and rainfall) with the seasons. Day 108 was approximately the start of winter in 2000, which was relatively mild.

Figures 5 through 8 show the mean macrocell currents in the concrete blocks reinforced with the 316LN, 304, 2205, and clad bars, respectively, with the different bar combinations listed in Table 1. For those blocks with either the 316LN, 304, 2205, or clad bars in both the top and bottom portions (i.e., blocks 316LN/316LN, 304/304, 2205/2205, and CB/CB), the mean macrocell current after 700 days (100 weekly cycles) of exposure was still practically indiscernible, even when plotted on an expanded scale (20X). Even the macrocell current of the blocks with clad bars with drilled holes through the cladding was likewise indiscernible. As Table 3 indicates, the mean macrocell currents ranged from only  $-0.0002$  to  $0.0004 \mu\text{A}/\text{cm}^2$ , which are virtually negligible considering that the error of measurements was  $\pm 0.0007 \mu\text{A}/\text{cm}^2$ . In comparison, the mean macrocell current of the CS/CS blocks was at least 1,000 times larger (see Table 3).

Interestingly, in the blocks reinforced with a combination of a bar other than carbon steel bars at the top and carbon steel bars at the bottom (e.g., 316LN/CS, 316LN (bent)/CS, 2205/CS), negative, or reversed, macrocell currents began to flow after some number of salt exposure

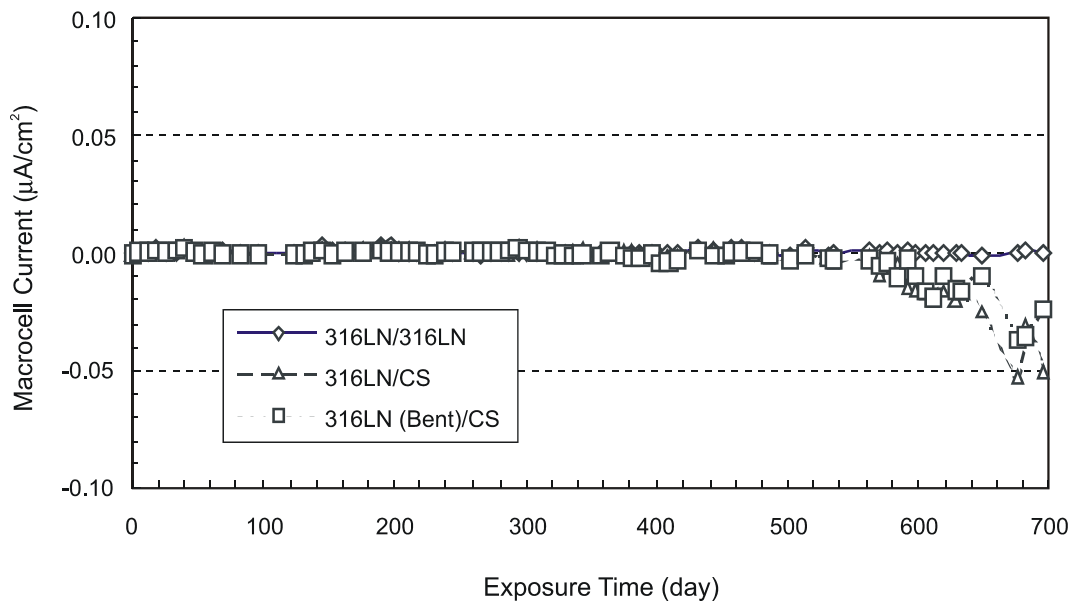


**Figure 5. Macrocell Currents of Test Concrete Blocks with 316LN Stainless Steel Bars in Various Bar Combinations.** The macrocell currents were normalized to the surface area of the top bars in the concrete blocks.

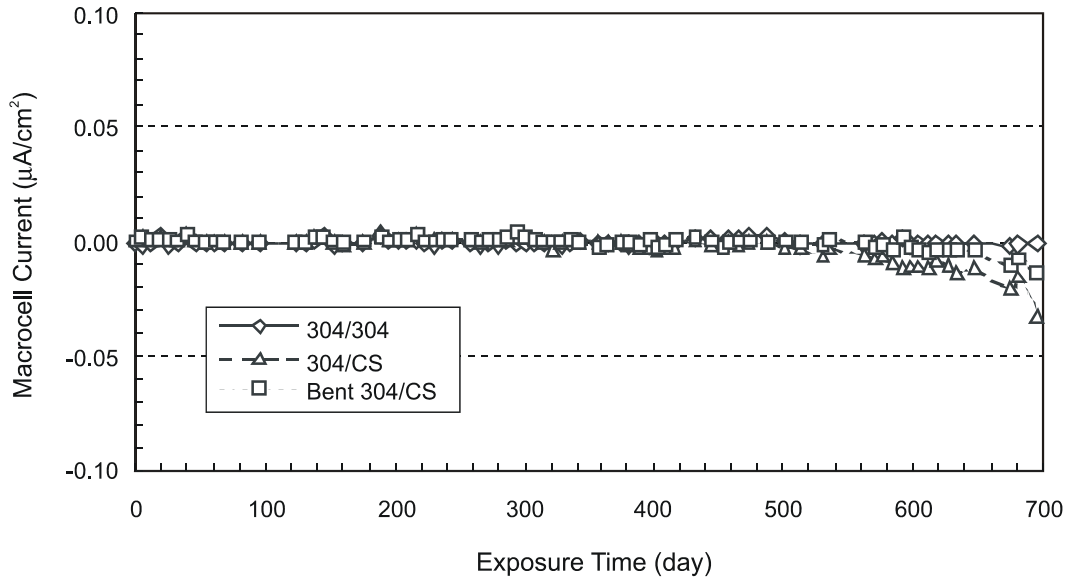


**Figure 6. Macrocell Currents of Test Concrete Blocks with 304 Stainless Steel Bars in Various Bar Combinations.** The macrocell currents were normalized to the surface area of the top bars in the concrete blocks.

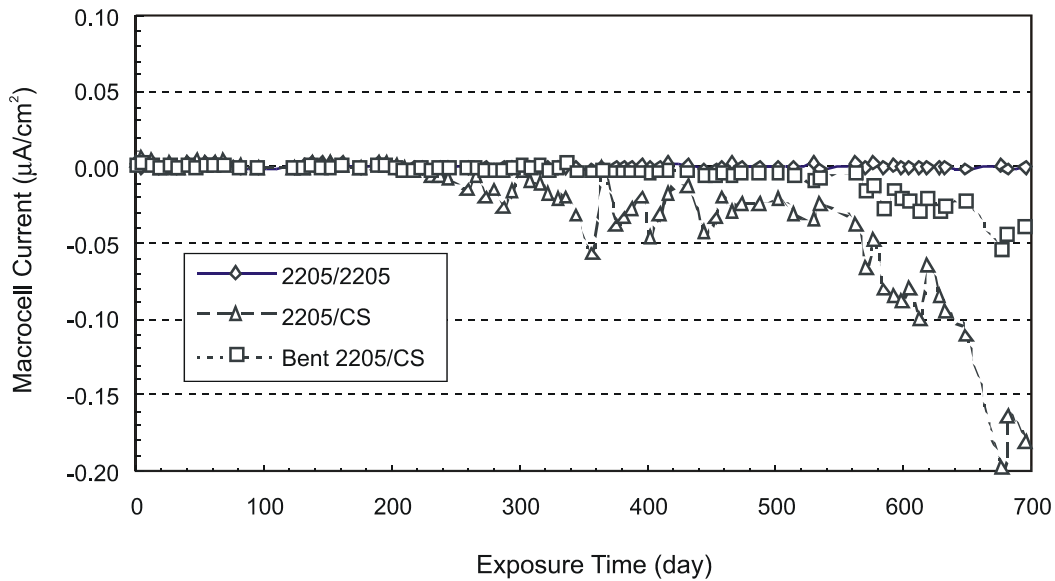


**Figure 7. Macrocell Currents of Test Concrete Blocks with 2205 Duplex Stainless Steel Bars in Various Bar Combinations.** The macrocell currents were normalized to the surface area of the top bars in the concrete blocks.

cycles. For example, as Figure 7 shows, blocks 2205/CS began to exhibit noticeable negative current flow at about 225 days. This phenomenon was not observed in the blocks where the top and bottom bars were of the same material. Except for expected fluctuations, this negative macrocell current continued to increase and reached  $-0.20 \mu\text{A}/\text{cm}^2$  in about 680 days. This is about 10 percent of the  $2.05 \mu\text{A}/\text{cm}^2$  positive macrocell current on day 294 for the CS (bent)/CS blocks (see Figure 4). Similarly, the 2205 (bent)/CS blocks began to exhibit a negative macrocell current, albeit after a longer salt exposure.

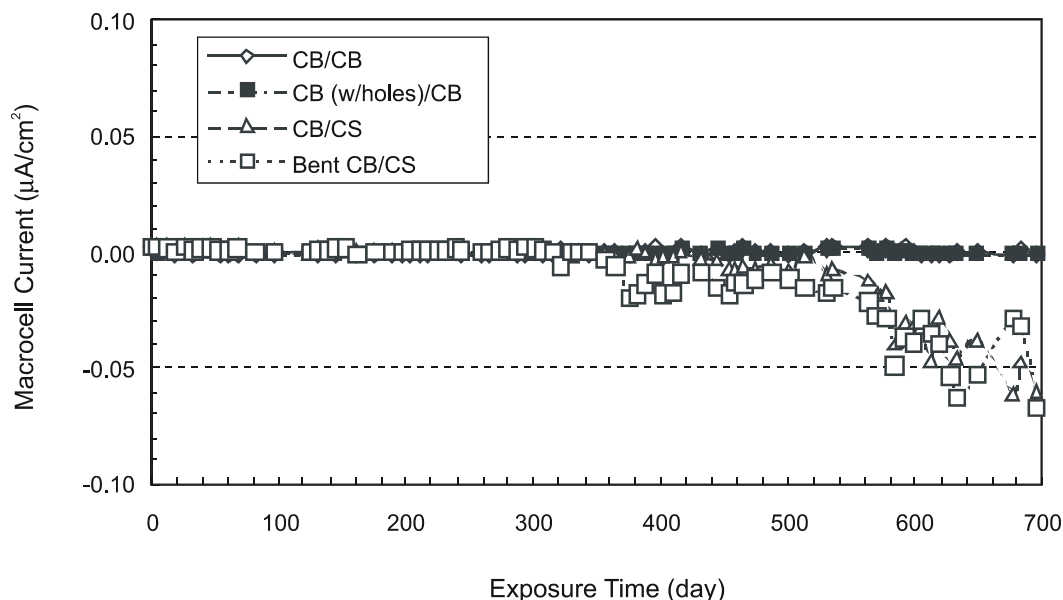


**Figure 8. Macrocell Currents of Test Concrete Blocks with Stainless Steel–Clad Bars, With or Without Holes Drilled Through Cladding, in Various Bar Combinations.** The macrocell currents were normalized to the surface area of the top bars in the concrete blocks.

Similarly, the CB/CS and CB (bent)/CS blocks began to exhibit a significant negative macrocell current after approximately 300 to 320 days (Figure 8). The 316LN/CS, 316LN (bent)/CS, 304/CS, and 304 (bent)/CS blocks also began exhibiting negative current flows at about 460 to 480 days. The time differences between the appearance of negative currents in the blocks were attributable to the heterogeneity in their permeability.

The occurrence of negative macrocell currents in the blocks in which carbon steel bars were used in the bottom portions indicates that chloride ions had reached the depth of the bottom bars to cause them to become more anodic than the relatively more corrosion-resistant bars at the top, even though the latter bars were surrounded by more chloride ions. This negative macrocell current flow means that the already corrosion-resistant 316LN, 304, 2205, and clad bars at the top of these blocks were being sacrificially protected by the corroding carbon steel bars at the bottom. This is confirmed by corrosion rate data for the bottom carbon steel bars in some of the blocks, which are presented in the next section.

### Corrosion Rates

As another electrochemical parameter for determining the existence of corrosion, the corrosion rate of all of the top bars was determined through measurement of their polarization resistance. Figures 9 through 13 show the corrosion rates for the bars during the 2 years of the investigation. Table 4 presents the mean corrosion rate for each type of bar for the different bar combinations. Rodriguez et al.<sup>4</sup> proposed the following interpretation of the significance of a measured steel-bar corrosion rate:

$I_{corr}$	less than	0.1 to 0.2 $\mu\text{A}/\text{cm}^2$	Steel passive
	between	0.2 and 0.5	Low corrosion
	between	0.5 and 1.0	Moderate corrosion
	greater than	1.0	Active corrosion

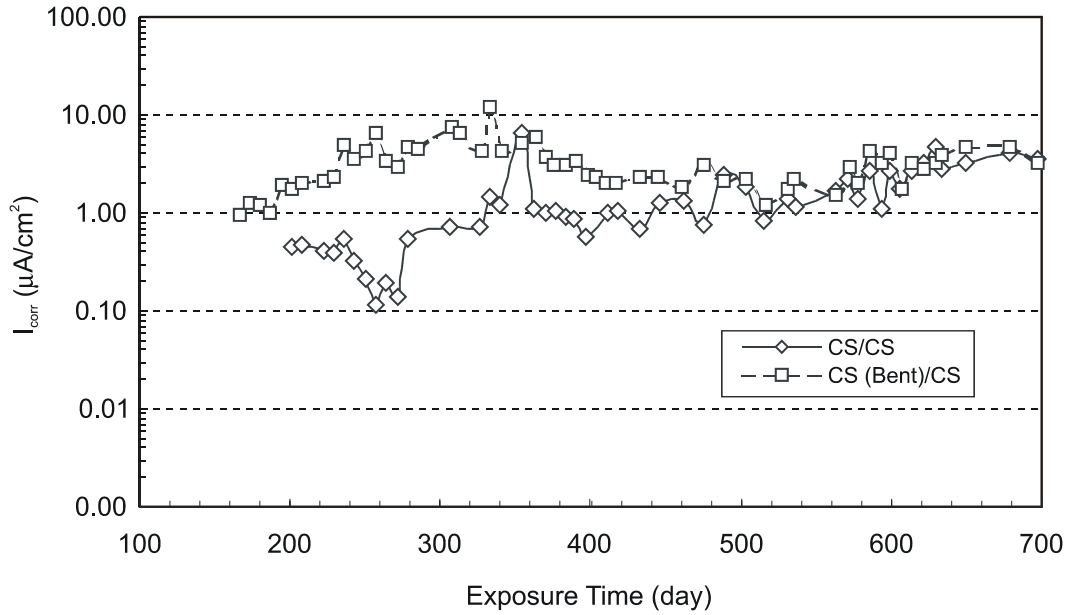


**Figure 9. Corrosion Rates of Carbon Steel Bars in Test Concrete Blocks.**

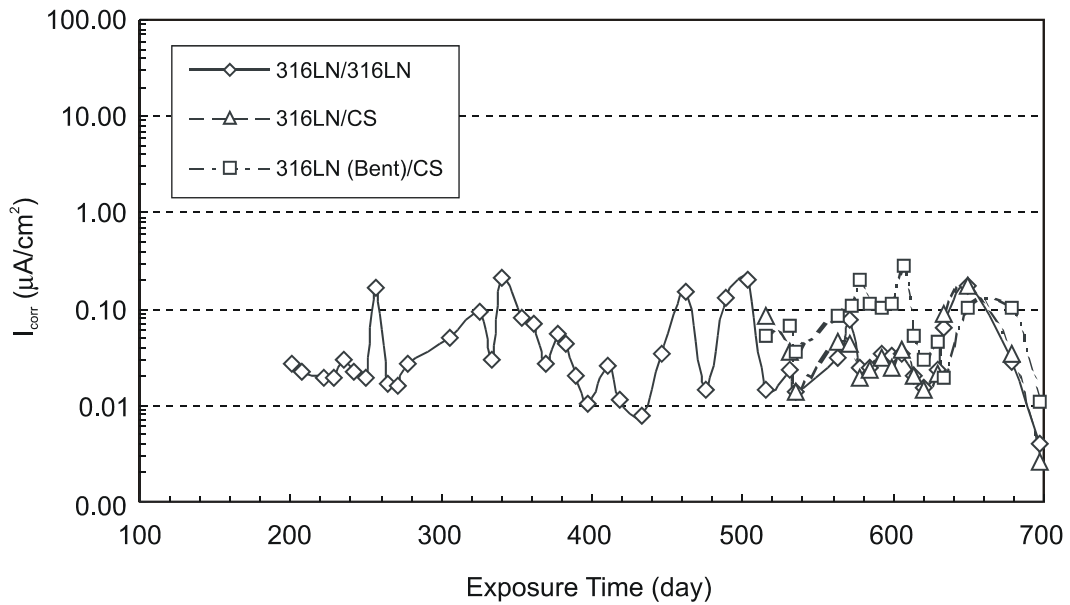


**Figure 10. Corrosion Rates of 316LN Stainless Steel Bars in Test Concrete Blocks.**

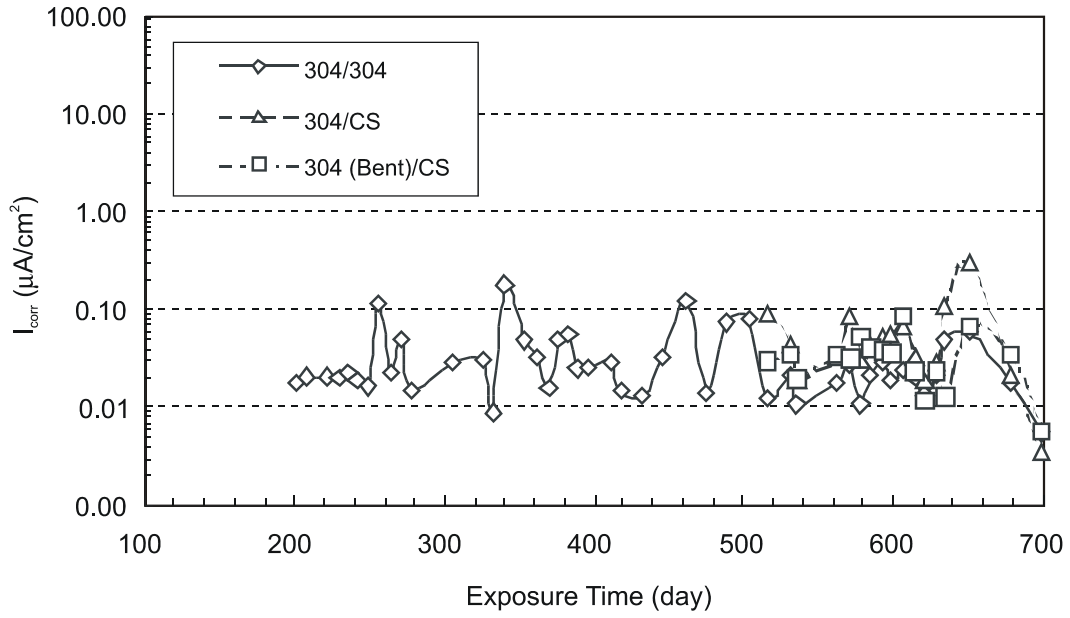


Figure 11. Corrosion Rates of 304 Stainless Steel Bars in Test Concrete Blocks

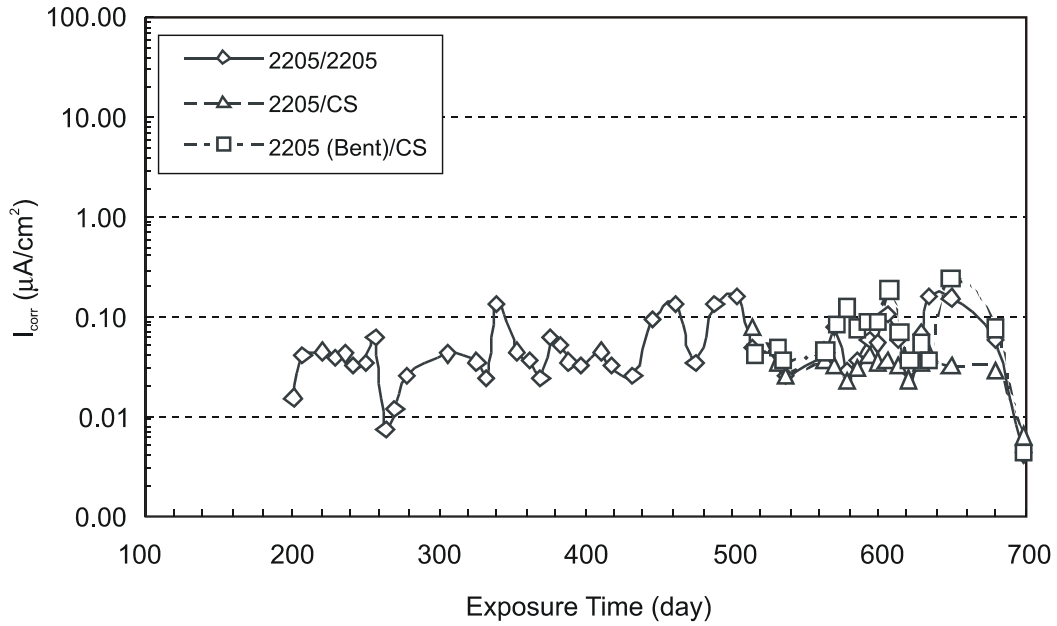


Figure 12. Corrosion Rates of 2205 Duplex Stainless Steel Bars in Test Concrete Blocks.

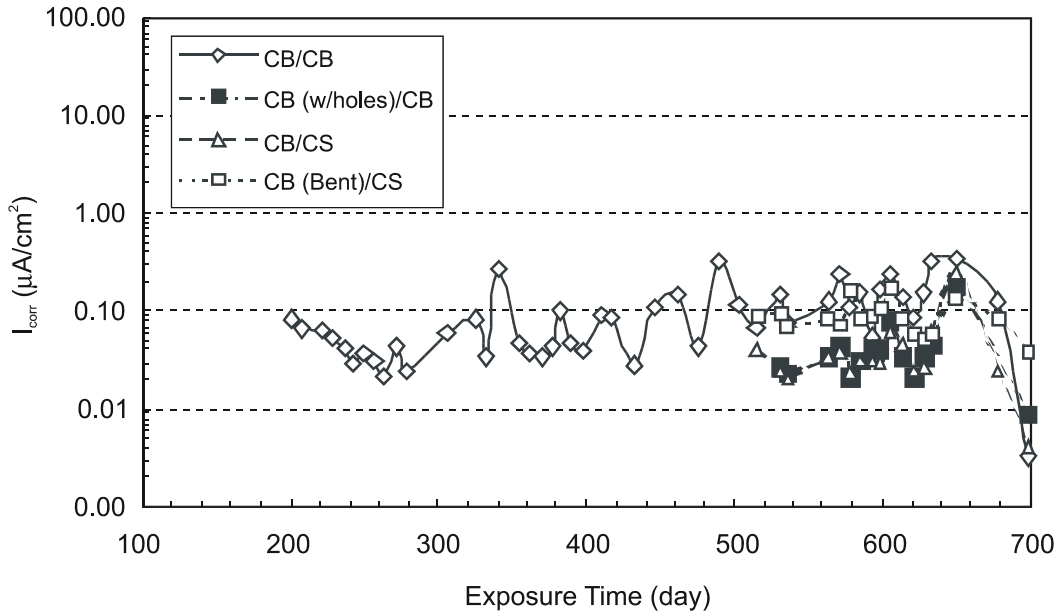


Figure 13. Corrosion Rates of Stainless Steel–Clad Bars in Test Concrete Blocks.

Table 4. Mean Corrosion Rates of Various Reinforcing Bars

Test Blocks (Bar Combination)	$I_{corr}$ ( $\mu\text{A}/\text{cm}^2$ )		Overall Mean
	Mean	Std. Dev.	
CS/CS	1.52	1.32	2.41
CS (bent)/CS	3.31	1.91	
316LN/316LN	0.05	0.05	0.09
316LN/CS	0.12	0.11	
316LN (bent)/CS	0.11	0.05	
304/304	0.03	0.03	0.07
304/CS	0.11	0.09	
304 (bent)/CS	0.07	0.06	
2205/2205	0.05	0.04	0.07
2205/CS	0.08	0.06	
220 (bent) /CS	0.08	0.04	
CB/CB	0.10	0.08	0.08
CB (w/holes)/CB	0.06	0.05	
CB/CS	0.12	0.05	
CB (bent)/CS	0.04	0.04	

CS = carbon steel bars; CB = clad bars.

According to these broad criteria for corrosion rate values, with mean corrosion rates of 1.52 and 3.31  $\mu\text{A}/\text{cm}^2$  for the straight and bent carbon steel bars, respectively, the bars were, as expected, actively corroding. This interpretation is consistent with the macrocell current for these two sets of test blocks and was supported by the typical visual signs of corrosion, such as rust stains and surface cracking, on the surface of many of the blocks, even at only 160 days of exposure. Figure 9 shows that the mean corrosion rate of the bent carbon steel bars was already

0.94  $\mu\text{A}/\text{cm}^2$  on the first day (day 166) corrosion rates were measured for the blocks with bent bars at the top. For the blocks with straight carbon steel bars, the mean corrosion rate was 0.45  $\mu\text{A}/\text{cm}^2$  on the first day (day 201). Further, as indicated in Figures 4 and 9, these bars appeared to have reached the corrosion level of the bent carbon steel bars after approximately 470 days of exposure.

In contrast, all the other types of bars were associated with extremely low corrosion rates (if any), even after approximately 700 days of severe exposure to salt. The lowest mean corrosion rate, 0.03  $\mu\text{A}/\text{cm}^2$ , was for the 304/304 blocks. The highest, 0.12  $\mu\text{A}/\text{cm}^2$ , was for the 316LN/CS blocks. Based on the criteria given previously, even the latter rate is considered to be passive or non-corroding.

With an overall mean corrosion rate for straight and bent bars of 2.41  $\mu\text{A}/\text{cm}^2$ , which is approximately 2 orders of magnitude greater than those for all other types of bars, there is no doubt that carbon steel was associated with the highest corrosion rate. Figure 14 shows the all-too-familiar concrete cracking and rust stain at the top of one of the blocks with straight carbon steel bars at both depths. For the other types of bars (not in combination with carbon steel bars), the ranking in terms of associated corrosion rates appears to be 2205 < 304 < clad < 316LN, in that increasing order. However, with standard deviations ranging from 0.03 to 0.11  $\mu\text{A}/\text{cm}^2$  for the various subsets of blocks, there is no clear indication that any one of these four types of bars was significantly more corrosion resistant than the others. Figure 15 shows the top of one of the blocks embedded with clad bars at both depths that was free of any outward sign of bar



**Figure 14. Top View of CS/CS (BB/BB) Concrete Block Showing Severe Corrosion of Top Carbon Steel Bar and Resulting Concrete Damage, After 700 Days.**



**Figure 15. Top View of Concrete Block With Clad Bars at Top And Bottom With No Sign of Corrosion, Even After 700 Days.** Blocks with stainless steel bars were similarly free of corrosion.

corrosion, even after 700 days of salt exposure; this is typical of the other concrete blocks embedded with the clad bars or any of the stainless steel bars.

It is noteworthy that the mean corrosion rate for the clad bars with the holes drilled through the cladding ( $0.06 \mu\text{A}/\text{cm}^2$ ) was not significantly different than those for the undamaged clad bars and the solid stainless steel bars. An ongoing, similar severe salt exposure of another series of blocks embedded with clad bars, each with a 2.5-cm cut through the cladding, has shown no discernible corrosion (after 364 days).<sup>6</sup> These observations perhaps indicate that small defects in the cladding, such as those intentionally introduced in the clad bars used in these investigations, may likely not be enough to adversely affect the protective function of the cladding, at least within the first 700 days. However, if cladding defects could occur during the manufacture of clad bars, the size of a defect at which the function of the cladding is significantly affected needs to be determined.

In the previous section, the appearance of negative or reversed macrocell currents in blocks reinforced with a combination of a more corrosion-resistant bar at the top and a carbon steel bar at the bottom after prolonged salt exposure was reported. It was stated that this implies that sufficient chloride ions had already reached the bottom carbon steel bars to cause them to become more anodic than the other bars at the top so that they were corroding. This was confirmed when subsets of these blocks (those with 2205 and clad bars) were turned upside down, on day 642, to allow measurement of the corrosion rates of the bottom carbon steel bars (see Table 5). With corrosion rates ranging from 1.15 to  $3.17 \mu\text{A}/\text{cm}^2$ , it is clear that the bottom

**Table 5. Corrosion Rates of Bottom Carbon Steel Bars in Selected Test Concrete Blocks**

on Exposure Day 642

Test Blocks (Bar Combination)	$I_{corr}$ ( $\mu\text{A}/\text{cm}^2$ )	
	Mean	Std. Dev
2205/CS	3.17	2.84
2205 (bent)/CS	1.51	0.65
CB/CS	1.15	1.75
CB (bent)/CS	1.51	1.35

CS = carbon steel bars; CB = clad bars.

carbon steel bars were already actively corroding. Even though no similar measurements were made on the subsets of blocks wherein either stainless steel 304 or 316LN was used in combination with carbon steel bars, it is expected that the corrosion rates of the bottom carbon steel bars in those blocks would also be high, although perhaps slightly lower.

### Open Circuit Potentials

Even though the open circuit potential does not indicate the status of a metal bar as well as macrocell current and corrosion rate do, it is still useful. When the potentials of carbon steel bars in concrete become more negative than  $-350$  mV (CSE), the probability that the bars are corroding is considered to be very high. As Figure 16 shows, the mean potentials of the bent carbon steel bars dropped to that level before 180 days and then continued to become even more negative, or anodic, until reaching a plateau of about  $-500$  to  $-550$  mV after 320 days. In contrast, the mean potential of the straight carbon steel bars was initially more positive, by at least  $100$  mV, than that of the bent carbon steel bars. Throughout the salt exposure, this potential steadily became more negative, reaching  $-350$  mV at approximately 355 to 360 days, and appeared to have approached the potential ( $-550$  mV) of their bent counterparts at about 700 days. This difference in the potentials parallels the difference between their macrocell currents

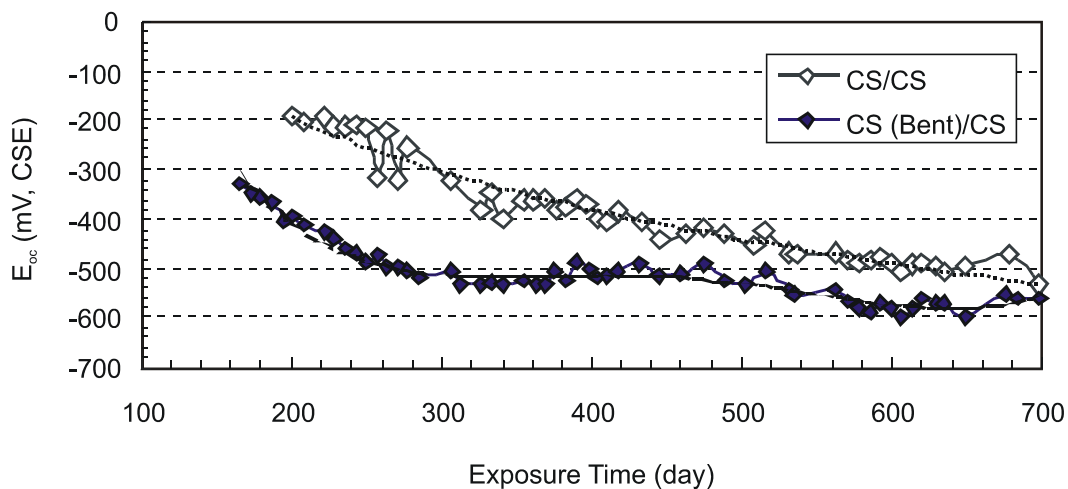
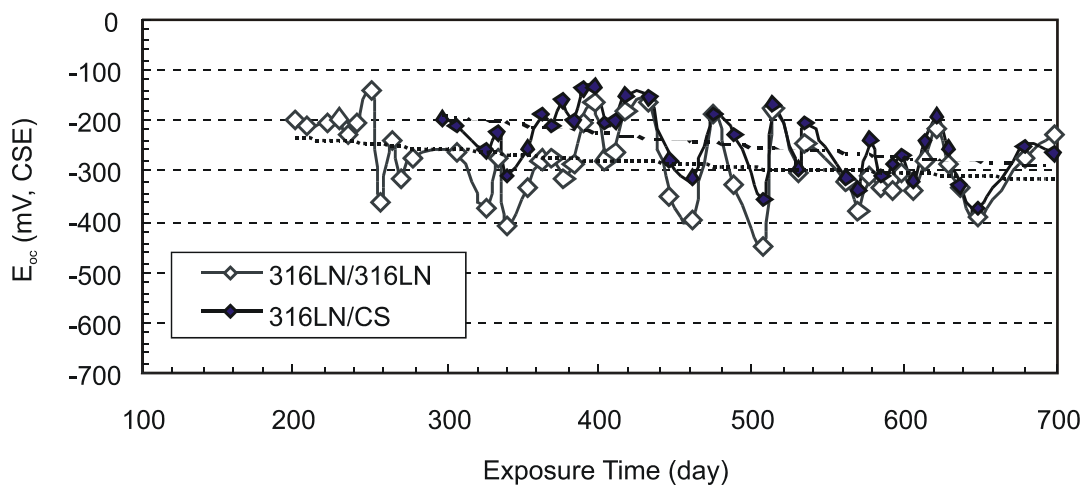


Figure 16. Potential of Carbon Steel Bars in Concrete Blocks With Straight or Bent Top Bars.

and corrosion rates (see Figures 4, 9, and 16); however, macrocell current, and perhaps even the corrosion rate, appeared to be a better early indicator of corrosion activity in steel bars. As a group, the averaged mean potential of the carbon steel bars in the two subsets of concrete blocks was  $-546$  mV at around 700 days, an indication that the bars were actively corroding.

Figures 17 through 20 show the open circuit potentials of the other types of bars. A common characteristic is an anodic trend, albeit at significantly slower rates than those for the carbon steel bars, with the exception of perhaps the 304 stainless steel bars, which remained virtually stable throughout the observation period from 201 to 700 days. The mean potentials at about 700 days were  $-249$ ,  $-212$ ,  $-247$ , and  $-211$  mV for the 316LN, 304, 2205, and clad bars, respectively. This means that these types of bars were 297 to 336 mV more cathodic than the carbon steel bars.



**Figure 17. Potential of 316LN Stainless Steel Bars in Concrete Blocks With Various Top and Bottom Bar Combinations.**

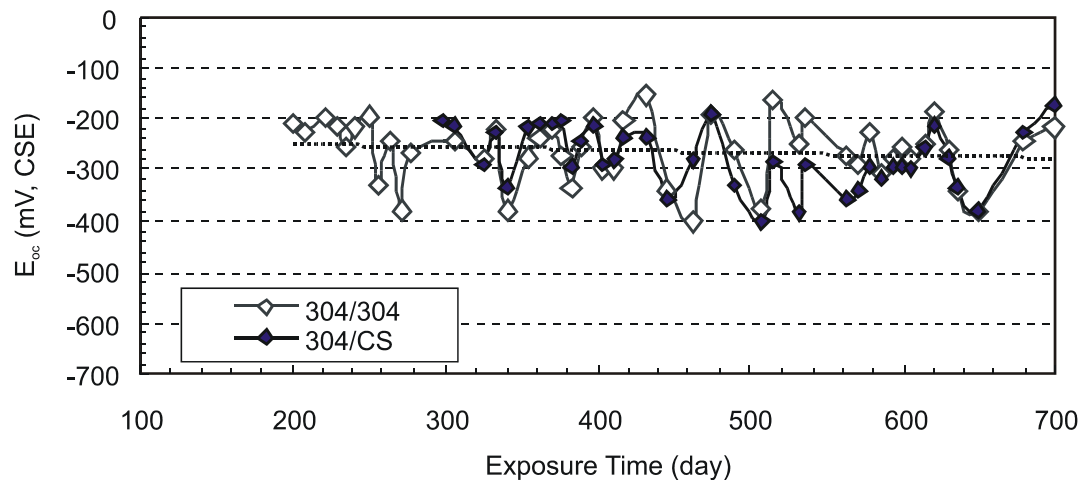


**Figure 18. Potentials of 304 Stainless Steel Bars in Concrete Blocks With Various Top and Bottom Bar Combinations.**

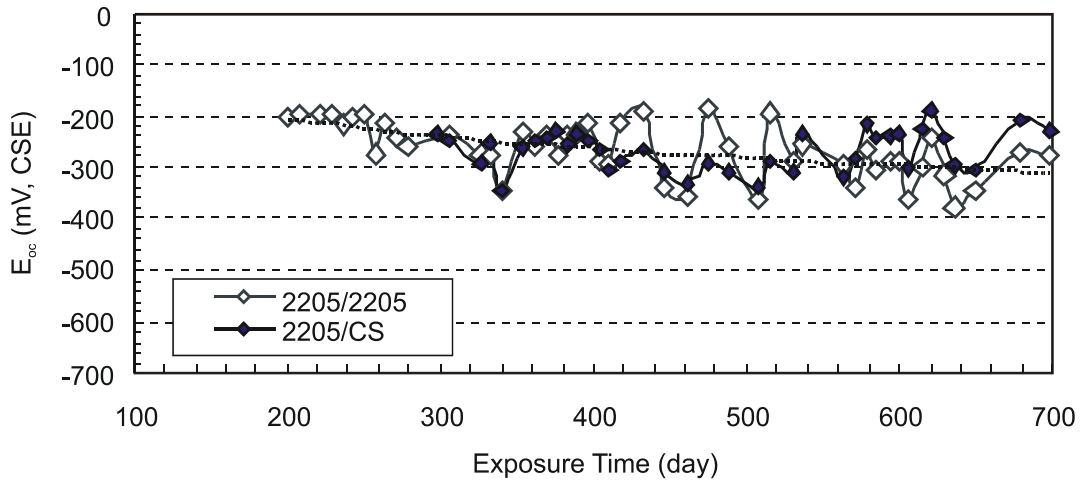


**Figure 19. Potential of 2205 Duplex Stainless Steel Bars in Concrete Blocks With Various Top and Bottom Bar Combinations.**

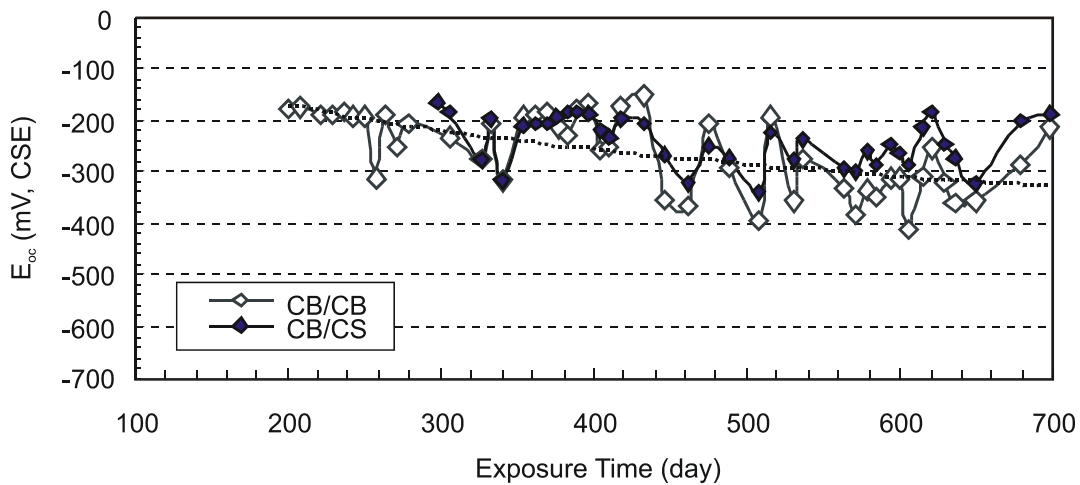


**Figure 20. Potential of Clad Bars in Concrete Blocks With Various Top and Bottom Bar Combinations.**

### Chloride Contents in Test Concrete Blocks

Figure 21 shows the mean chloride concentrations in the blocks at different depths and exposure times, as determined by analysis of the ground concrete samples obtained from 10 randomly selected test concrete blocks, i.e., 2 from each group of blocks. From the best-fit curves for these chloride ion distributions, the mean chloride ion concentration in the blocks at different exposure times can be estimated for a specific depth. Figure 22 shows the estimated mean chloride concentration at different exposure times for the depth of 33 mm, which was the depth of the top-mat bars.

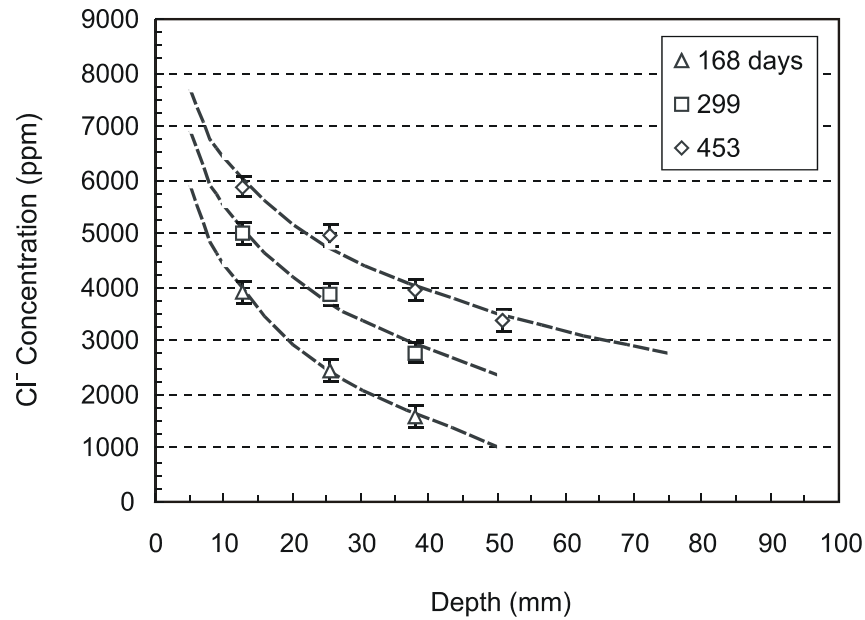


**Figure 21. Mean Chloride Ion Concentrations at Different Depths of Test Concrete Blocks After Different Exposure Times.**

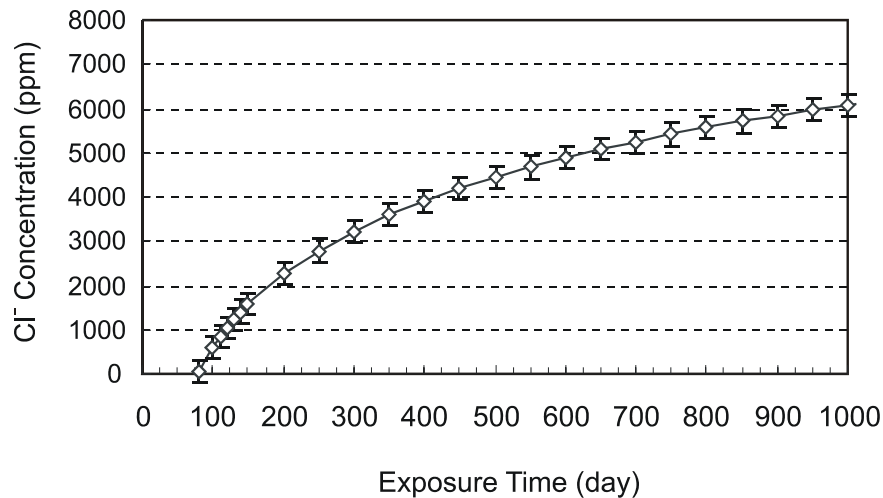


**Figure 22. Estimated Mean Chloride Ion Concentrations as Function of Exposure Time, at Depth of Top Bars (33 mm) in Test Concrete Blocks.**

It was noted earlier that the macrocell current of the blocks with the bent carbon steel bars began to rise steadily after approximately 90 days of exposure, indicating the onset of corrosion (see Figure 4). It can be estimated from Figure 22 that the mean chloride concentration in the concrete blocks at that time would be approximately  $350 \pm 100$  ppm. This value is in good agreement with the widely accepted chloride threshold level for corrosion of reinforcing steel in concrete, which is 330 ppm (1.32 lb/yd<sup>3</sup>).

In contrast, all the electrochemical parameters, including macrocell current, corrosion rate, etc., recorded after even approximately 700 days of exposure indicated that all the other types of bars remained passive. Figure 22 shows that at 700 days the mean chloride concentration around these bars would be approximately  $5200 \pm 100$  ppm ( $20.8$  lb/yd<sup>3</sup>). This means that the clad bars, including those with 3-mm holes drilled through the cladding, and all the stainless steel bars tolerated 15 times more chloride than the carbon steel bars were able to tolerate. This is in agreement with the findings reported recently by McDonald et al. that the threshold levels of 304 and 316 stainless steels were 15 and 24 times, respectively, higher than that of carbon steel.<sup>5</sup>

The findings in this investigation are consistent with those obtained in the companion investigation of most of these same metallic bars in simulated pore solutions with various concentrations of chlorides.<sup>3</sup> Potentiostatic polarization of these metallic bars in solutions indicated that chloride thresholds for corrosion initiation in the solid 316LN bars and the clad bars were as high as 16 times and 11 times, respectively, that of carbon steel bars, with the difference attributed to differences in alloy composition.<sup>3</sup> In addition, the repassivation potential for the clad bars, as long as the clad layer was not penetrated, was equivalent to that of the solid 316LN bars.<sup>3</sup>

This and the cited companion investigation represent attempts to shed light on the corrosion initiation characteristics of clad bars in comparison with those of particular stainless steel bars and carbon steel bars. Work is underway to investigate the propagation characteristics of these bars, both in solution and in concrete, once corrosion has been initiated. Autopsy of many of the concrete blocks used in the current investigation will be performed in the near future to allow for actual microscopic examination of the nature of the corrosion, if any, on the different types of bars.

## CONCLUSIONS

- *Within the 2-year time frame of this investigation, the stainless steel cladding appeared to have provided protection to the carbon steel core to such an extent that the clad bars exhibited the same high corrosion resistance as the three solid stainless steel bars (316LN, 304, and 2205) investigated. Although the carbon steel bars began corroding early during weekly accelerated and severe exposures to salt, the clad bars and the stainless steel bars showed no signs of corrosion during the 2-year term of the study. In addition, the clad bars, just like the three stainless steel bars, tolerated a chloride ion content in the concrete estimated to be at least 15 times more than that tolerated by the carbon steel bars. The data obtained in this investigation essentially confirm the preliminary data on clad bars reported by McDonald et al.<sup>1</sup> As part of a study<sup>6</sup> of the corrosion propagation characteristics of clad bars, 316LN bars, and bars made of two new alloys, the weekly salt exposure of the test concrete blocks used in this investigation, particularly those reinforced with the clad bars and the stainless steels, is being continued. In addition, some of these concrete blocks and those with the embedded newer bars will be autopsied so that the corrosion propagation characteristics of each of these new bars, should corrosion occur, can be determined.*

- *The presence of the 3-mm holes drilled through the stainless steel cladding had no adverse effect on the underlying carbon steel core during the duration of this study.* As noted earlier, an ongoing similar salt exposure of another series of concrete blocks embedded with clad bars, each with 2 2.5-cm cut through the cladding, has yielded similar results after 364 days. These data may simply indicate that if defects in the cladding can occur, they must be larger than a threshold size before the carbon steel core is adversely effected. This, of course, begs the question: What could this threshold size be? Perhaps an investigation of this issue is warranted.
- *It would be risky to use a combination of a more corrosion-resistant but more expensive bar in the top-mat reinforcement of a bridge deck and a cheaper but corrosion-susceptible carbon steel bar in the bottom mat.* This investigation demonstrated, perhaps for the first time, that sufficient chloride ions will eventually reach the bottom mat of reinforcement to cause the bottom carbon steel bars to corrode before the more corrosion-resistant top bars (see Figures 23 and 24).



**Figure 23. Side View of Concrete Block With 316LN Stainless Steel Bars at Top and Carbon Steel Bars at Bottom.** Notice the rust stain and cracking at the lower right corner attributable to corrosion on the bottom carbon steel bars.



**Figure 24. Side View of Concrete Block With 316LN Stainless Steel Bars at Both Top and Bottom.** No sign of corrosion is present, even after 650 days of severe weekly cycles of salt ponding and drying.

## ACKNOWLEDGMENTS

The authors express their gratitude to various entities or individuals for providing the test samples: to Acerinox USA, Inc., for providing the 316LN and the 2205 duplex stainless steels; to the now-defunct Civil Engineered Products Limited, South Yorkshire, U.K., for providing the 304 stainless steel bars; and to Frank Pianca of the Ontario Ministry of Transportation, Ontario, Canada, for providing the clad bars. Appreciation is extended to Cesar Apusen and other members of the Research Council for their valuable assistance.

## REFERENCES

1. McDonald, D.B., Pfeifer, D.W., and Blake, G.T. *The Corrosion Performance of Inorganic-, Ceramic-, and Metallic-Clad Reinforcing Bars and Solid Metallic Reinforcing Bars in Accelerated Screening Tests*. FHWA-RD-96-085. Federal Highway Administration, Washington, D.C., 1996.
2. Nurnberger, U., Beul, W., and Onuseit, G. Corrosion Behavior of Welded Stainless Reinforcing Steel in Concrete. *Otto Graf Journal*, Vol. 4, pp. 225-259, 1993.
3. Scully, J.R., Marks, C.A., and Hurley, M.F. *Testing of Selected Metallic Reinforcing Bars for Extending the Service Life of Concrete Bridges: Testing in Solutions*. FHWA/VTRC 03-CR11. Virginia Transportation Research Council, Charlottesville, 2002.

4. Rodriguez, J., Ortega, L.M., and Garcia, A.M. Assessment of Structural Elements with Corroded Reinforcement. *Proceedings of the International Conference on Corrosion and Corrosion Protection of Steel in Concrete*. Sheffield Academic Press, University of Sheffield, Sheffield, England, July 1994.
5. McDonald, D.B., Pfeifer, D.W., and Sherman, M.R. *Corrosion Evaluation of Epoxy-Coated, Metallic-Clad and Solid Metallic Reinforcing Bars in Concrete*. FHWA-RD-98-153. Federal Highway Administration, Washington, D.C., 1998.
6. Clemeña, G.G., and Scully, J.R. *Work Plan: Investigation of the Corrosion Propagation Characteristics of New Metallic Reinforcing Bars*. Virginia Transportation Research Council, Charlottesville, 2001.